NASA TECHNICAL MEMORANDUM

NASA TM X-2556

NASA TM X-2556

A PROCEDURE FOR PREDICTING INTERNAL AND EXTERNAL NOISE FIELDS OF BLOWDOWN WIND TUNNELS

by

Robert N. Hosier
Langley Directorate,
U.S. Army Air Mobility R&D Laboratory

and

William H. Mayes
Langley Research Center

NATIONAL AERONAUTICS AND SPACE ADMINISTRATION • WASHINGTON, D. C. • MAY 1972

1. Report No.	2. Government Accession No.	3. Recipient's Catalog No.
NASA TM X-2556		

4. Title and Subtitle	5. Report Date
A PROCEDURE FOR PREDICTING INTERNAL AND EXTERNAL NOISE FIELDS OF BLOWDOWN WIND TUNNELS	May 1972
	6. Performing Organization Code

7. Author(s)	8. Performing Organization Report No.
Robert N. Hosier, Langley Directorate, U.S. Army Air Mobility R&D Laboratory; and William H. Mayes	L-8132
	10. Work Unit No.
9. Performing Organization Name and Address	132-80-01-04
NASA Langley Research Center Hampton, Va. 23365	11. Contract or Grant No.
	13. Type of Report and Period Covered
12. Sponsoring Agency Name and Address	Technical Memorandum
National Aeronautics and Space Administration Washington, D.C. 20546	14. Sponsoring Agency Code

15. Supplementary Notes

16. Abstract

The noise generated during the operation of large blowdown wind tunnels is considered. Noise calculation procedures are given to predict the test-section overall and spectrum level noise caused by both the tunnel burner and turbulent boundary layer. External tunnel noise levels due to the tunnel burner and circular jet exhaust flow are also calculated along with their respective cut-off frequency and spectrum peaks. The predicted values are compared with measured data, and the ability of the prediction procedure to estimate blowdown-wind-tunnel noise levels is shown.

17. Key Words (Suggested by Author(s))	18. Distribution Statement
Blowdown wind tunnel Noise prediction Turbulent-boundary-layer noise Combustion noise Jet noise	Unclassified – Unlimited

19. Security Classif. (of this report)	20. Security Classif. (of this page)	21. No. of Pages	22. Price*
Unclassified	Unclassified	23	$3.00

*For sale by the National Technical Information Service, Springfield, Virginia 22151

A PROCEDURE FOR PREDICTING INTERNAL AND EXTERNAL NOISE FIELDS OF BLOWDOWN WIND TUNNELS

By Robert N. Hosier
Langley Directorate, U.S. Army Air Mobility R&D Laboratory

and William H. Mayes
Langley Research Center

SUMMARY

A study has been made to devise a procedure for predicting the internal (test-section) and external noise fields generated by large blowdown wind tunnels. Noise calculation procedures are given to predict the test-section overall and spectrum level noise caused by both the tunnel burner and turbulent boundary layer. External tunnel noise levels due to the tunnel burner and circular jet exhaust flow are also calculated along with their respective cut-off frequency and spectrum peaks. The external wind-tunnel overall sound pressure levels and spectrum levels predicted by this procedure compare favorably with existing experimental data.

INTRODUCTION

The increase of airplane design speeds to supersonic and hypersonic regimes has precipitated the need to construct increasingly larger blowdown wind tunnels in which to test scale models of airplane components. In order to define the model test environment and to minimize environmental pollution, accurate prediction of the internal and external acoustic fields generated by blowdown wind tunnels has become necessary.

The purpose of this paper is to systematize the available information into a procedure for predicting the internal (test-section) and external noise fields generated by large blowdown wind tunnels. Included in these procedures are techniques for predicting the overall levels and spectral content of both the internal and external noise fields as well as the associated directivity patterns. Structural radiation of sound from the exhaust diffuser or combustion sections was assumed to be of secondary importance since such radiation can be effectively minimized by the massive structures and the addition of damping materials. Flow separation at the tunnel exit was also ignored. It was further assumed that only a small portion of each tunnel run would be spent with the control valve in other than the full-open position. Thus, valve noise, which under some conditions can

be significant, was not considered in this study. Also included in this paper are a discussion of the sources of tunnel noise, a detailed listing of the assumptions made in developing the procedure, a sample tunnel noise calculation, and a limited comparison of predicted tunnel noise levels and experimental data.

SYMBOLS

A	cross-sectional area, meters^2
c	speed of sound, meters per second
DI	directivity index, decibels
d	physical diameter of tunnel section, meters
f	frequency, hertz
f_b	burner noise cut-off frequency, hertz
f_j	external jet noise spectrum peak frequency, hertz
f_o	turbulent-boundary-layer cut-off frequency, hertz
f_t	cut-off frequency of burner noise in test section, hertz
H	enthalpy per unit mass in burner section, joules per kilogram
I	acoustic intensity
I_{ref}	acoustic intensity for flame with velocity $V = V_{ref}$
M	local free-stream Mach number, V/c
NPWL	normalized sound power level as determined from figure 8, decibels $\left(\text{re } 10^{-12} \text{ watt}\right)$
N_{Str}	Strouhal number, fd/V

OAPWL	overall sound power level, decibels
OASPL	overall sound pressure level, decibels (re 0.00002 newton per meter^2)
P	acoustic power, watts
P_o	reference power, 10^{-12} watt
PWL	sound power level, 10 log P/P_o, decibels
PWL(f)	sound power level at frequency f, decibels
p	overall rms pressure for burner noise or fluctuating-turbulent-boundary-layer noise, newtons per meter^2
p_o	reference pressure, 0.00002 newton per meter^2
R	distance from source, meters
SPL	sound pressure level, 20 log p/p_o, decibels
SPL(f)	sound pressure level at frequency f, decibels
TBL	turbulent boundary layer
t_{ISA}	static temperature of air at ICAO standard atmosphere, 288.5 kelvins
t_o	ambient static temperature, kelvins
V	local free-stream flow velocity, meters per second
V_{ref}	reference flow velocity, 15 meters per second
w	mass-flow rate, kilograms per second
x	distance from inception of turbulence (assume 3.04 m or distance from leading edge, whichever is greater), meters

δ^* boundary-layer-displacement thickness, $(1.6 \times 10^{-3})x$ for $0 < M < 2$ and $(4.0 \times 10^{-3})x$ for $2 < M < 4$, meters

θ azimuthal angle about tunnel exit in ground plane, degrees

ρ local gas density, kilograms per meter^3

ρ_{ISA} density of air at ICAO standard atmosphere, 1.224996 kilograms per meter^3

ρ_j fully expanded jet density, kilograms per meter^3

ρ_o ambient density, kilograms per meter^3

Subscripts:

b at tunnel burner section

e at tunnel exhaust section

ext outside environment

j jet

sp power spectrum level or sound pressure spectrum level

t at tunnel test section

th at tunnel throat

SOURCES OF BLOWDOWN-WIND-TUNNEL NOISE

The major sources of blowdown-wind-tunnel noise are of aerodynamic origin and include the turbulent-boundary-layer flow fields within the tunnel and the turbulent mixing of the jet exiting to the quiescent atmosphere. If the tunnel has elevated temperature capability then the noise due to the combustion process may also have to be considered. Estimation procedures, based on many research studies made relative to aircraft operations, have been developed for predicting the noise levels due to the turbulent-boundary-layer and jet-exhaust flow. However, few studies have been made and little is known

about the noise produced by the combustion process. References 1 to 6 are representative of the prediction techniques that have been developed for the aerodynamic noise sources. Reference 1 presents a theoretical model for the prediction of the turbulent-boundary-layer intensity at supersonic speeds. Empirical formulas are presented for the intensity, spectrum, and cross spectrum of the boundary-layer fluctuation. Reference 2 presents a review of turbulent-boundary-layer data from flight and wind-tunnel tests. A review of low-velocity jet noise data is presented in reference 3. Also, a prediction scheme for the coaxial jet noise of turbofan engines is developed and compared with full-scale turbofan noise measurements in reference 3. In reference 4 the directivity of subsonic jet noise is defined and reference 5 presents measured supersonic wind-tunnel exhaust sound pressure levels and directivities. Among other things, reference 6 defines sound pressure levels and spectra for subsonic jet engines.

References 7 and 8 contain information relative to combustion noise. Reference 7 discusses the generation mechanisms and characteristics of the noise associated with combustion. The dipole and monopole contributions to the sound field by the velocity and entropy turbulences are shown. Empirical data are also presented of the spectral distribution of flame noise intensity. In reference 8, after a critical review of previous combustion noise theories, another combustion noise theory is developed.

The purpose of this paper is to systematize the preceding information into a procedure for predicting the internal and external noise fields of blowdown wind tunnels. Included in these procedures are techniques for predicting the overall levels and spectral content of both the internal and external noise fields as well as the associated directivity patterns. Structural radiation of sound from the exhaust diffuser or combustion sections was assumed to be of secondary importance since such radiation can be effectively minimized by the massive structures and the addition of damping materials. Flow separation at the tunnel exit was also ignored. It was further assumed that only a small portion of each tunnel run would be spent with the control valve in other than the full-open position. Thus, valve noise, which under some conditions can be significant, was not considered in this study.

The sources of test-section noise considered were the burner and the turbulent boundary layer (TBL). Similarly, the outside noise environment had two important sources: the burner and the jet exhaust flow. These sources of noise are indicated in figure 1 along with the main wind-tunnel sections.

The burner noise in the test section can be detrimental to a model or panel specimen by causing induced structural vibrations which may interfere with aerodynamic measurements or may fatigue the skin of the specimen. The noise in the area surrounding the tunnel exit is of concern to tunnel operating personnel and to adjacent community

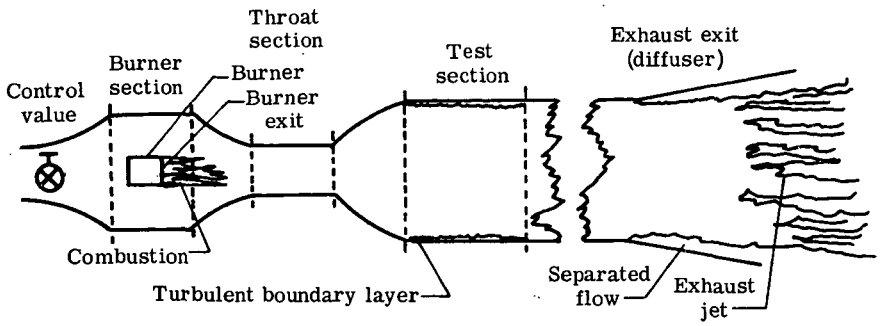

Figure 1.- Conceptual model of blowdown wind tunnel with main tunnel components and noise sources indicated.

areas. A technique for predicting the noise levels in these areas is desirable in the planning stages of new wind tunnels and when noise controls are being considered for existing tunnels.

PROCEDURES FOR PREDICTING NOISE

Noise Prediction Methods and Assumptions

This phase of the study involved the development of a method for predicting test section and external noise generated by blowdown wind tunnels. The methods and assumptions used for predicting the noise from the sources discussed in the preceding section were as follows. In reading this section the reader should make reference to figures 1 and 2.

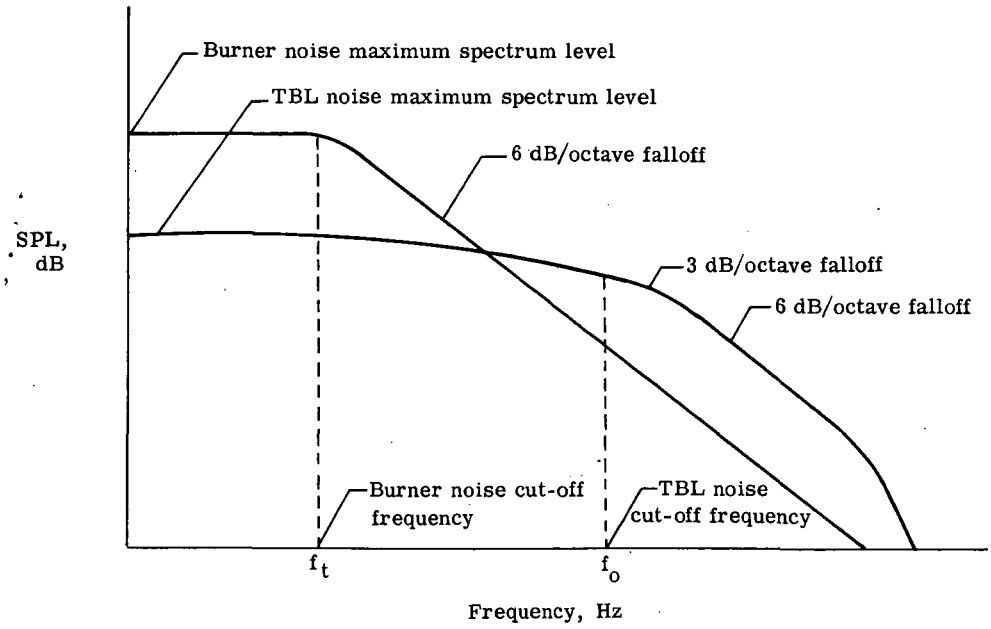

Figure 2.- Definition of burner and TBL spectrum levels and cut-off frequencies.

A. Test-section burner noise

1. One percent of the total mechanical power in the burner was assumed converted to acoustic power as shown by the following equation:

$$P_b = 0.01Hw$$

2. All acoustic energy generated by the combustion process was assumed to radiate toward the throat section.

3. The acoustic power transmitted to the test section and the outside environment was assumed to be that portion which was incident on the open throat portion of the tunnel; that is,

$$P_{th} = P_t = P_b \frac{A_{th}}{A_b}$$

4. Plane wave acoustic theory was used and continuity of acoustic power from the throat to the test section was assumed. From this assumption the overall rms pressure was calculated in the test section by

$$p_t^2 = P_t\left(\frac{\rho c}{A}\right)_t$$

5. The shape of the pressure spectrum due to the burner noise was determined by the method of reference 7. Figure 3, plotted after data from this reference,

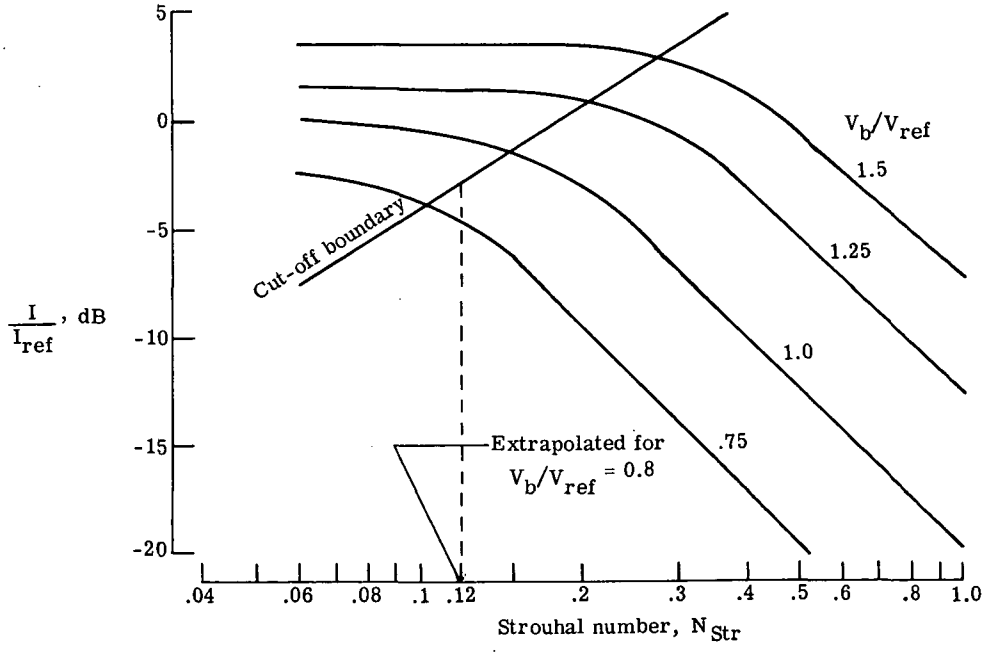

Figure 3.- Curves used to determine burner noise-spectrum shape.

shows burner noise intensity divided by I_{ref} plotted against the Strouhal number as a function of the ratio V_b/V_{ref} where V_b is the gas velocity at the burner exit. This figure was used to determine the burner noise cut-off frequency and spectrum shape as defined by the cut-off boundary. After determining the location of the V_b/V_{ref} curve for the burner under consideration, the intersection with the cut-off boundary determined the burner Strouhal number. Since the burner diameter d and flow velocity V_b were known, the cut-off frequency f_b was determined from the Strouhal number. The portion of the burner noise spectrum at frequencies above the cut-off boundary was not assumed to contribute to the overall noise level.

6. The standard Doppler correction was applied to the entire pressure spectrum including the cut-off frequency; that is,

$$f_t = f_b(1 + M_t)$$

7. The maximum pressure spectrum level SPL_{sp} was calculated from

$$SPL_{sp} = OASPL - 10 \log f_t = 20 \log \frac{p_t}{p_o} - 10 \log f_t$$

B. Turbulent-boundary-layer pressures at test-section wall

1. The overall rms pressure and pressure level generated at the test-section wall surfaces by the turbulent boundary layer were calculated by the following equations:

$$p_{TBL} = 0.001(\rho V^2)_t$$

$$OASPL_{TBL} = 20 \log p_{TBL}$$

2. The pressure spectrum shape was assumed to be that given in figure 4 (from ref. 2).

3. The turbulent-boundary-layer pressure spectrum cut-off frequency was calculated by the following equation from reference 2:

$$f_o = 0.1 \frac{V_t}{\delta^*}$$

4. The turbulent-boundary-layer maximum spectrum level was determined by adding $OASPL_{TBL} - 10 \log f_o$ to the ordinate of figure 4.

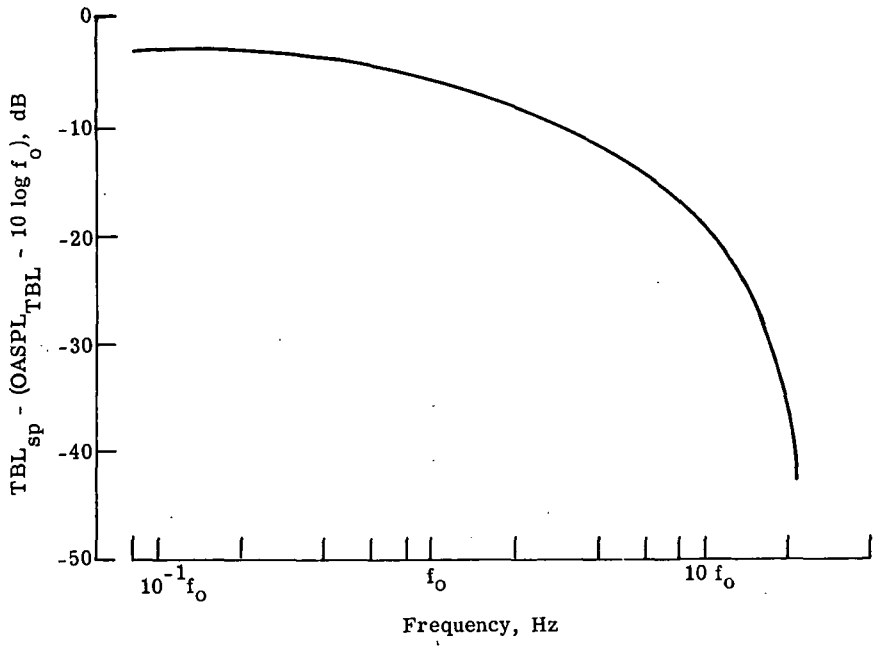

Figure 4.- Chart for estimating boundary-layer pressure spectra. TBL spectrum level in 1-Hz bands is obtained by adding the quantity $OASPL_{TBL}$ - 10 log f_o to ordinate values.

5. The contribution of the spectrum beyond f_o to the OASPL was neglected.

C. Outside noise due to burner

1. All acoustic power incident to the test section was assumed to radiate from the tunnel exit.

2. Three dB were added to the total burner power at the exit to account for radiation into a hemisphere.

3. The method of reference 9 was used to calculate OASPL at distance R from the exit as follows:

$$OASPL = PWL - 20 \log R - 10.8 \text{ dB}$$

4. The burner noise was assumed to have the same directivity as the jet flow at the tunnel exit. (See D3.)

5. The procedures of A6 and A7 were used to apply Doppler corrections to the burner cut-off frequency and to determine the maximum burner noise spectrum level.

D. Outside noise due to jet flow

1. In calculating the outside OASPL due to subsonic exit jet flow, figure 5 (data from ref. 3) was used. To obtain OASPL for a subsonic exit jet the quantity

$$10 \log\left(\frac{\rho_j \rho_o}{\rho_{ISA}^2} A_j \frac{t_o^2}{t_{ISA}^2} \frac{1}{R^2}\right)$$

must be added to the ordinate.

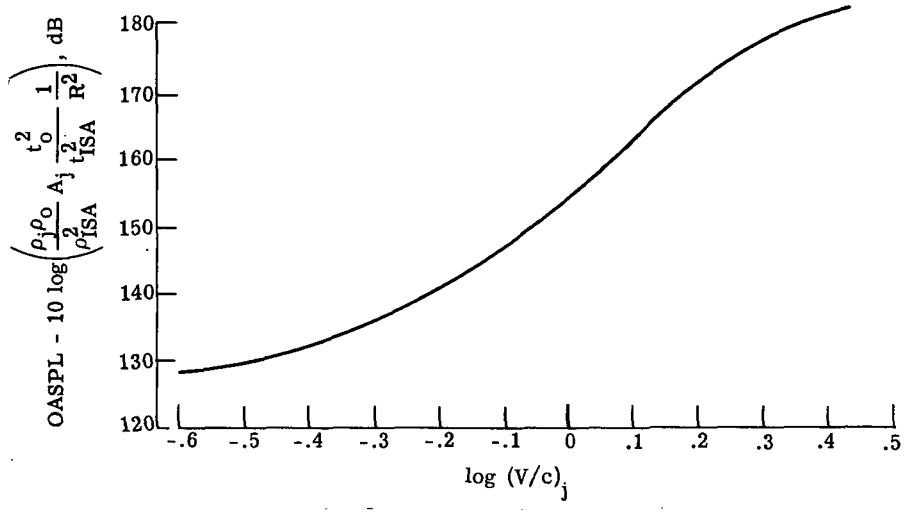

Figure 5.- Subsonic jet noise OASPL.

2. For supersonic flow the acoustic power was calculated according to the relation

$$P_j = \frac{1}{2}\% \text{ of mechanical power} = \left(2.5 \times 10^{-3}\right)\left(\rho A V^3\right)_e$$

The method of C3 was then used to calculate OASPL.

3. Three dB must be added to OASPL to correct for radiation into a hemisphere.

4. The OASPL obtained from these operations (D1 and D2) was adjusted for directivity according to reference 4 for subsonic exit jets and according to reference 5 for supersonic exit jets. Figure 6 shows the directivity indices from these references. The directivity index was for a circular jet and hence was assumed to be symmetric about the tunnel axis with the directivity pattern centered at the tunnel exit. (0^o is in the downstream direction.)

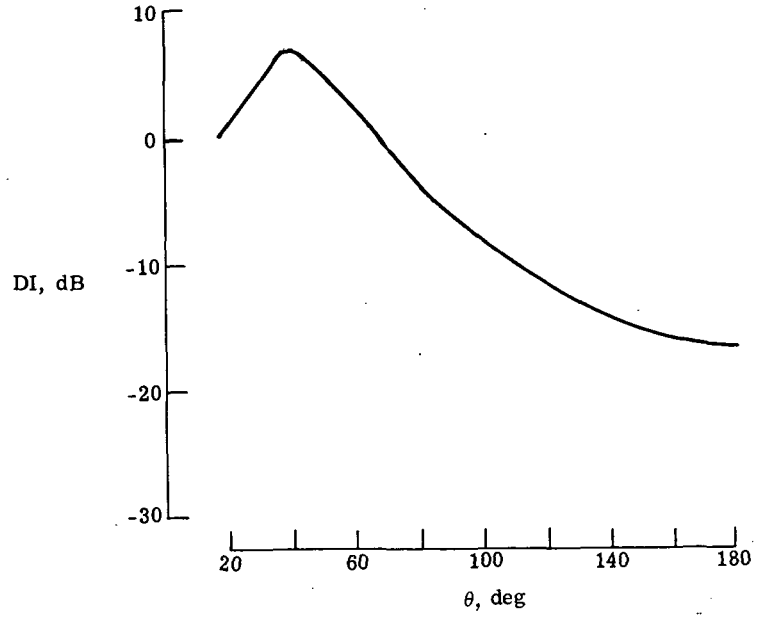

(a) Subsonic directivity index.

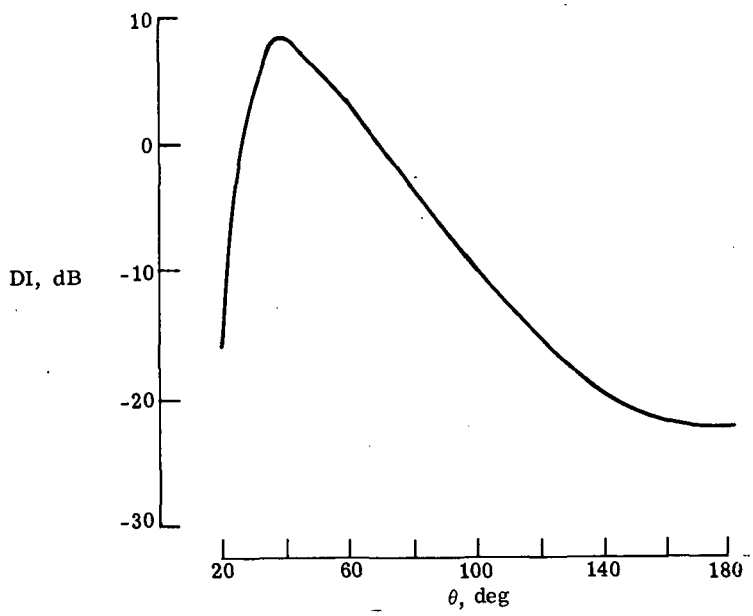

(b) Supersonic directivity index.

Figure 6.- Directivity indices.

5. The spectrum peak frequency for a subsonic exit jet should be calculated by using

$$f_j = 0.2\left(\frac{V}{d}\right)_e$$

as given in reference 6.

6. To compute the spectrum shape and levels for a subsonic exit jet, figure 7, from reference 6, should be used. This figure shows the octave band SPL relative to OASPL plotted against Strouhal number. The numbers shown in figure 7 should be added to OASPL to obtain the correct spectrum levels.

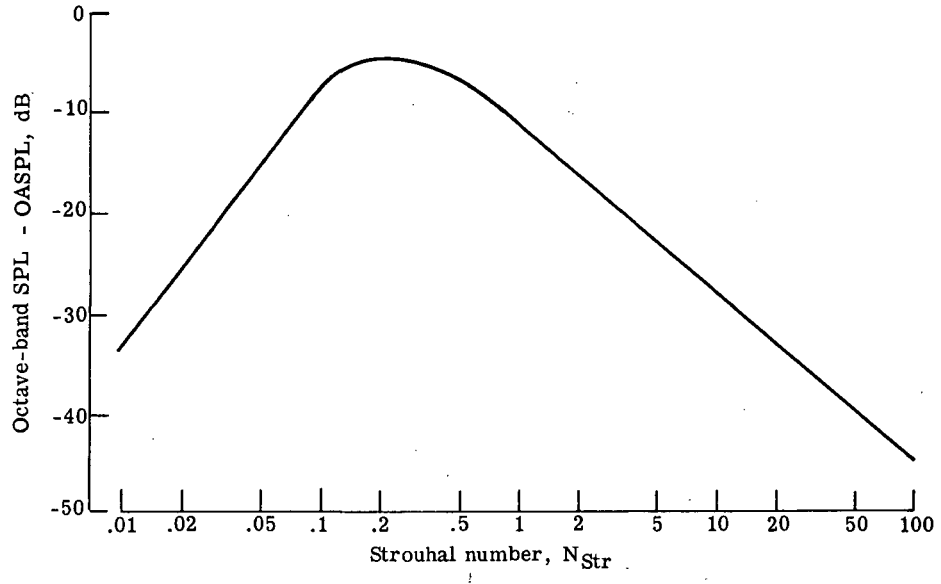

Figure 7.- Octave band subsonic exit jet noise as a function of Strouhal number.

7. The spectrum peak frequency for a supersonic exit jet should be calculated with

$$f_j = 0.02\left(\frac{V}{d}\right)_e$$

as given in reference 10.

8. To compute the spectrum shape and levels for a supersonic exit jet, figure 8, from reference 10, was used. This figure shows the normalized relative sound power spectrum level NPWL as a function of Strouhal number N_{Str}. In order to obtain the correct spectral distribution, figure 8 and the following equation were used.

$$PWL_j(f) = NPWL + OAPWL_j + 10 \log\left(\frac{d}{V}\right)_e + DI$$

9. Both the subsonic and supersonic spectra were adjusted for atmospheric absorption effects by the use of the empirical curves shown in figure 9, from reference 11. These data, for 288.15 K and 50 percent relative humidity, show both classical and molecular losses. The contribution of both losses must be summed at any given frequency.

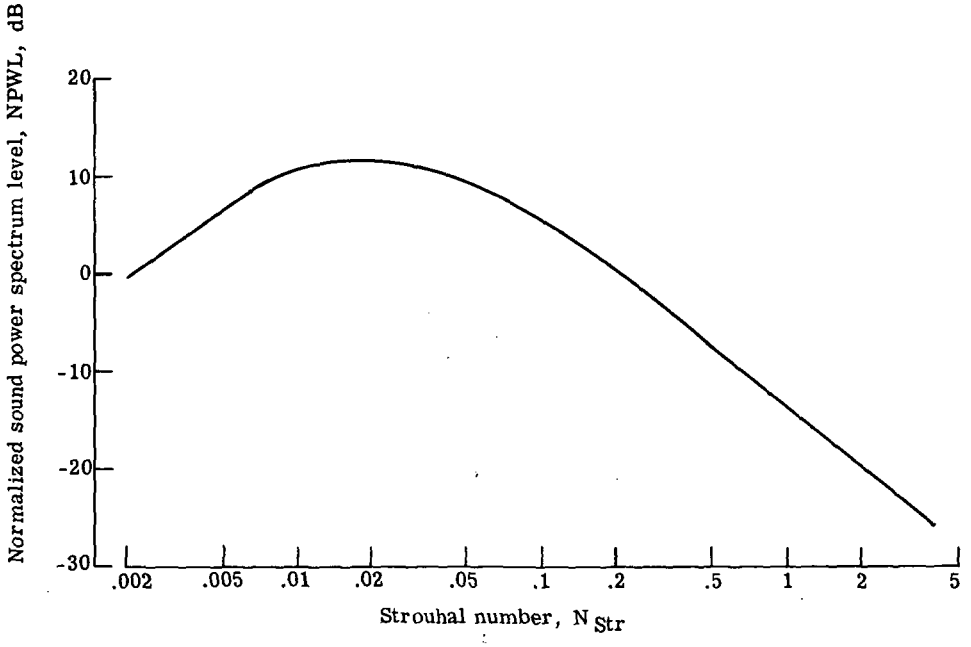

Figure 8.- Normalized sound power spectrum as function of Strouhal number for supersonic exit jet.

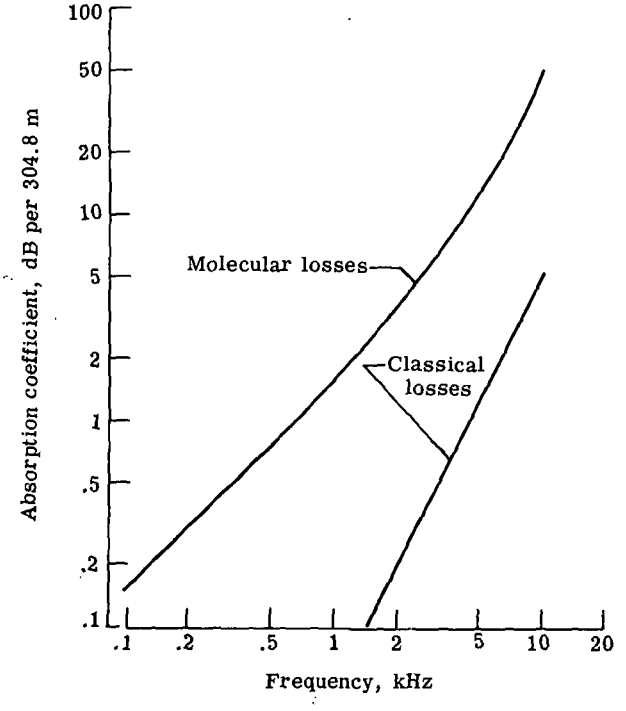

Figure 9.- Atmospheric absorption curves.

Sample Calculation for Tunnel B

Geometric and airflow parameters for the wind tunnels are given in table I.

TABLE I.- GEOMETRIC AND AIRFLOW PARAMETERS FOR WIND TUNNELS

Tunnel	Location	Physical diameter, d, m	Cross-sectional area, A, m^2	Density, ρ, kg/m^3	Flow velocity, V, m/sec	Free-stream temperature, K	Speed of sound, c, m/sec	Enthalpy at burner, H, J/kg	Mass-flow rate, w, kg/sec
A	Throat	1.19	1.121	4.16	456	518	456	---------	2.55×10^3
	Test section	2.47	4.877	.21	896	222	298	---------	2.55
	Exhaust exit[a]	3.66 (2.47)	10.498 (4.830)	.86	792	259	322	---------	2.55
B	Combustor	0.91	0.657	43.09	12	2056	884	2.67×10^6	3.46×10^2
	Throat	.14	.016	26.43	823	1833	823	---------	3.46
	Test section	2.44	4.672	.04	2073	222	286	---------	3.46
	Exhaust exit[a]	4.18 (2.07)	13.656 (3.409)	.07	1798	217	297	---------	4.31

[a] Number in parentheses refers to free jet.

A. Test-section burner noise

1. Acoustic energy generated by combustion process in burner:

$$P_b = 0.01Hw = 0.01\left(2.67 \times 10^6\right)\left(3.46 \times 10^2\right) = 9.19 \times 10^6$$

2. Acoustic power transmitted to test section:

$$P_{th} = P_t = P_b \frac{A_{th}}{A_b} = \left(9.19 \times 10^6\right)\frac{1.6 \times 10^{-2}}{6.57 \times 10^{-1}} = 2.23 \times 10^5$$

3. Power level (PWL) of acoustic energy transmitted to test section:

$$OAPWL_t = 10 \log \frac{P_t}{P_o} = 10 \log \frac{2.23 \times 10^5}{10^{-12}} = 173$$

4. rms acoustic pressure in test section:

$$p_t = \left[P_t\left(\frac{\rho c}{A}\right)_t\right]^{1/2} = \left[\left(2.23 \times 10^5\right)\left(4 \times 10^{-2}\right)\frac{2.86 \times 10^2}{4.672}\right]^{1/2} = 7.22 \times 10^2$$

5. Burner noise overall rms sound pressure level (OASPL):

$$\text{OASPL} = 20 \log \frac{p_t}{p_o} = 20 \log = \frac{7.22 \times 10^2}{2 \times 10^{-5}} = 151$$

6. Burner pressure spectrum: For tunnel B, $\frac{V_b}{V_{ref}} = 0.8$. From figure 3, the curve for $\frac{V_b}{V_{ref}} = 0.8$ can be seen to cross the cut-off boundary at $N_{Str} = 0.12$. Thus,

$$f_b = 0.12\left(\frac{V}{d}\right)_b = 0.12 \frac{12}{9.1 \times 10^{-1}} = 1.58$$

Correcting for the Doppler shift in the test section gives

$$f_t = f_b(1 + M_t) = 1.58(1 + 7.24) = 13$$

7. Maximum pressure spectrum level:

$$\text{SPL}_{sp} = \text{OASPL} - 10 \log f_t = 151 - 10 \log 13 = 140$$

B. Turbulent-boundary-layer pressures at test-section wall

1. Pressure generated at test-section wall due to turbulent flow:

$$p_{TBL} = 0.001\left(\rho V^2\right)_t = 10^{-3}\left(4 \times 10^{-2}\right)\left(2.073 \times 10^3\right)^2 = 1.68 \times 10^2$$

2. Overall sound pressure level of turbulent boundary layer:

$$\text{OASPL}_{TBL} = 20 \log \frac{p_{TBL}}{p_o} = 20 \log \frac{1.68 \times 10^2}{2 \times 10^{-5}} = 138$$

3. Cut-off frequency, from reference 2:

$$f_o = 0.1 \frac{V_t}{\delta^*} = 0.1 \frac{2.073 \times 10^3}{1.216 \times 10^{-2}} = 1.7 \times 10^4$$

This method is valid for flow velocities up to Mach 4.

4. Maximum TBL spectrum level:

$$\text{SPL}_{sp} = \text{OASPL}_{TBL} - 10 \log f_o = 138 - 10 \log\left(1.7 \times 10^4\right) = 96$$

C. Outside noise due to burner

1. External burner acoustic power: from part A3, the power level of the burner noise is 173 dB.

2. Correction for radiation into a hemisphere: 3 dB must be added to results of A3 as

$$\text{OAPWL} = 173 + 3 = 176$$

3. Distance and directivity corrections applied to the results of C2: the distance correction is

$$\text{OASPL} = \text{OAPWL} - 20 \log R = 176 - (20 \log 304.8 + 10.8) = 176 - 60 = 116$$

The directivity correction is taken from figure 6(b). Thus at 304.8 m from the exit of tunnel B, the sound pressure level due to the burner at 20° azimuthal increments are shown in the following table:

θ, deg	OASPL, dB
20	100
40	124
60	119
80	112
100	107
120	100
140	97
160	94
180	94

4. Burner noise cut-off frequency: This is the combustor cut-off frequency adjusted for Doppler effects. From A6, $f_b = 1.58$ Hz; adjusting for Mach number effects gives

$$f_{b,ext} = f_b\left(1 + M_e\right) = 1.58\left(1 + \frac{1.798 \times 10^3}{2.97 \times 10^2}\right) = 11$$

D. Outside noise due to jet flow

1. Since the tunnel has supersonic exit conditions, the overall acoustic power generated by jet flow is calculated from

$$P_j = \frac{1}{2}\% \text{ of mechanical power} = \left(2.5 \times 10^{-3}\right)\left(\rho A V^3\right)_e$$

$$= \left(2.5 \times 10^{-3}\right)\left(7 \times 10^{-2}\right)3.41\left(1.798 \times 10^3\right)^3 = 3.5 \times 10^6$$

2. Overall jet power level $\left(OAPWL_j\right)$:

$$OAPWL_j = 10 \log \frac{P_j}{P_o} = 10 \log \frac{3.5 \times 10^6}{10^{-12}} = 185$$

3. Correcting D2 for radiation into a hemisphere gives

$$OAPWL_j = 185 + 3 = 188$$

4. Correcting for distance and directivity as in C3 gives the following values at 304.8 m from the exit of tunnel B:

θ, deg	OASPL, dB
20	112
40	136
60	131
80	124
100	119
120	112
140	109
160	106
180	106

5. The normalized sound power spectrum is shown in figure 8. From this figure the spectrum peak frequency is calculated as

$$f_j = 0.02\left(\frac{V}{d}\right)_e = 2 \times 10^{-2}\left(\frac{1.798 \times 10^3}{2.07}\right) = 17$$

6. The jet sound pressure spectrum peak at 304.8 m from the tunnel exit and at an angle of 20^o is calculated from the equation,

$$SPL(f) = NPWL(f) + OAPWL_j + 10 \log\left(\frac{d}{V}\right)_e - (20 \log R + 10.8) + DI$$

$$SPL(17) = 12 + 188 + 10 \log \frac{2.07}{1.798 \times 10^3} - 60 - 16 = 95$$

7. Adjustments for 1/3-octave band spectrum and atmospheric attenuation from references 9 and 11 are shown in figure 10.

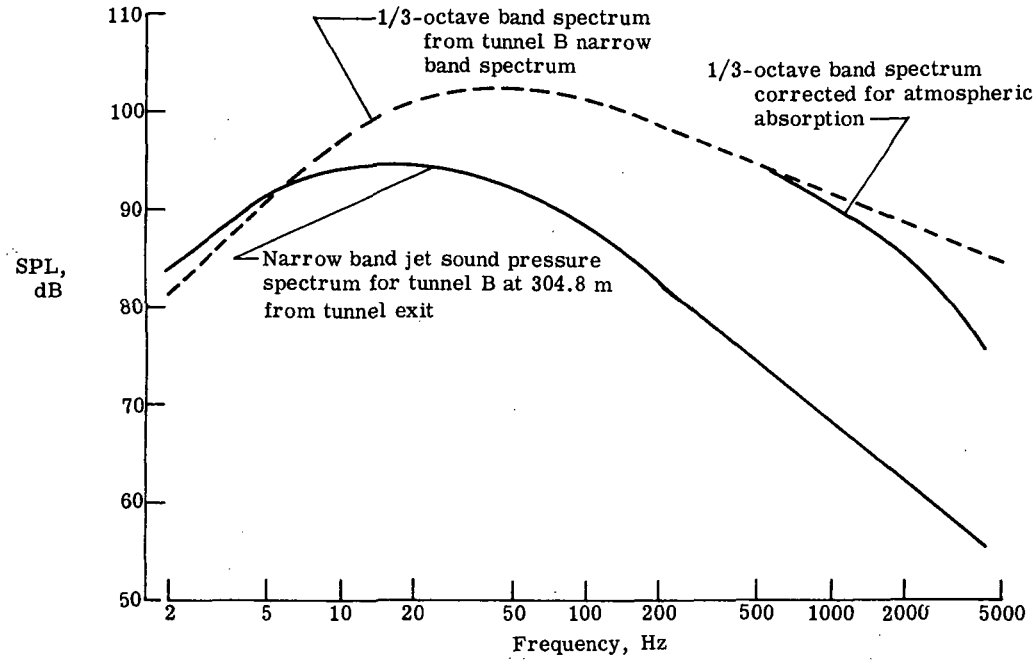

Figure 10.- Adjustment of tunnel B narrow band exit jet spectrum for atmospheric absorption and conversion to 1/3-octave band spectrum.

TUNNEL NOISE PREDICTIONS

The noise prediction outlined in the preceding section was applied to two separate blowdown wind tunnels. Table I presents the geometric and airflow parameters for each of the tunnels. Test-section and external noise calculations for both of the tunnels were similar in format with one exception: tunnel B used a gas burner to heat the inflow whereas tunnel A employed no burner.

Table II shows the noise and spectrum estimates for tunnels A and B. Table II(a) presents the predicted burner noise levels and turbulent-boundary-layer noise levels at the test-section wall. In addition, the predicted cut-off frequency and maximum spectrum level for the two sources are shown. In using table II(a) reference should again be made to figure 2 for definition of the maximum spectrum levels and cut-off frequencies. Table II(b) shows the estimated external noise levels at 304.8 m from the tunnel exit for 9 azimuthal positions about the tunnel, with 0^{o} being the downflow direction. Also given are the spectrum peak frequency for the external jet noise and the spectrum cut-off frequency for the external burner noise.

TABLE II.- NOISE AND SPECTRUM ESTIMATES

(a) Estimated internal noise levels at test-section wall

	Burner		TBL	
	Tunnel A	Tunnel B	Tunnel A	Tunnel B
OASPL, dB	---	151	138	138
Maximum spectrum level, dB	---	140	100	96
Cut-off frequency, Hz	---	13	7350	17 000

(b) Estimated external noise levels at 304.8 m from tunnel exit

θ, deg	Burner OASPL, dB, for –		Jet OASPL, dB, for –	
	Tunnel A	Tunnel B	Tunnel A	Tunnel B
20	---	100	114	112
40	---	124	138	136
60	---	119	133	131
80	---	112	126	124
100	---	107	121	120
120	---	100	114	112
140	---	97	111	109
160	---	94	108	106
180	---	94	108	106
Cut-off frequency, Hz	---	11	---	---
Spectrum peak frequency, Hz	---	---	6	17

For tunnel A, table II indicates that the TBL is the only source of test-section noise. The OASPL due to TBL is 138 dB with a cut-off frequency of 7350 Hz. The maximum predicted TBL sound pressure spectrum level was then predicted to be 100 dB. The external noise for tunnel A was due to jet noise exclusively since tunnel A had no burner. The directivity pattern has a maximum in the 40^{o} direction of 138 dB at 304.8 m. The spectrum peak frequency was predicted to be 6 Hz.

Because tunnel B used a burner to preheat the inflow the noise levels in the test section are significantly higher than for tunnel A. In the test section the burner noise far exceeded the TBL noise in overall level (13 dB) and in maximum spectrum level (44 dB). The burner noise cut-off frequency was predicted to be 13 Hz and the TBL cut-off frequency was predicted to be 17 000 Hz. Thus the TBL noise is the main contributor to the response of a wall-mounted test specimen at frequencies above 13 Hz. Conversely, structural response at frequencies below 13 Hz is controlled mainly by the burner noise.

Outside tunnel B the jet noise exceeded the burner noise by 12 dB in overall level with maximum intensity in the 40^{o} direction. (See table II.) The external jet spectrum peak frequency was predicted to be 17 Hz, whereas the external burner noise had a cut-off frequency of 11 Hz.

EXPERIMENTAL MEASUREMENTS

Since few data were available on the noise generated by the tunnels used for this study, the external noise generated by tunnel B was measured to evaluate the accuracy of the tunnel noise predictions. An array of microphones was placed at ground level every 20^{o} in a semicircular pattern 304.8 m from the tunnel exit. The first microphone was placed 20^{o} off the downstream axis (that is, no microphone was placed at 0^{o}) and the last microphone position was located 180^{o} from the exit. All microphones were of a commercially available piezoelectric ceramic type with frequency responses flat to within ±3 dB over the frequency range of 20 Hz to 12 000 Hz. The outputs of all microphones at each station were recorded on multichannel FM magnetic tape recorders. The entire sound measurement system was calibrated at 1000 Hz in the field before and after the acoustic measurements by means of commercially available discrete frequency calibrators. The data records were played back from the tape to obtain the overall sound pressure level time histories and 1/3-octave band spectra.

The microphone stations at angles 20^{o} to 100^{o} were in open-field, grassy areas with undulating terrain. The stations at angles 120^{o} to 180^{o} were located near hard reflecting surfaces such as parking lot pavement and buildings.

COMPARISON OF PREDICTED AND MEASURED RESULTS

Figure 11(a) presents predicted and measured data for tunnel A. The predicted values were obtained by the methods of this paper whereas the measured data were obtained from reference 5 and adjusted to 304.8 m. At all positions the predicted values of OASPL are seen to be no more than 2 dB greater than the measured overall levels. No far-field spectral information is presented in reference 5 so that comparison of the predicted and measured spectrum levels and shapes is not possible.

Figure 11(b) presents a comparison of the estimated and measured OASPL from all microphone positions at 304.8 m from tunnel B. It can be seen that four of the nine levels were predicted exactly; one was underpredicted by 1 dB; and the ones at the remaining four locations were underpredicted by 4 to 9 dB. The large overprediction at 40^{o} is attributed to the rapid rate of change of the directivity index in the 30^{o} to 50^{o} range, as is shown in figure 6(b). The differences between prediction and measurement at the 120^{o}, 140^{o}, and 160^{o} locations are believed due to reflections from large buildings near the measuring stations.

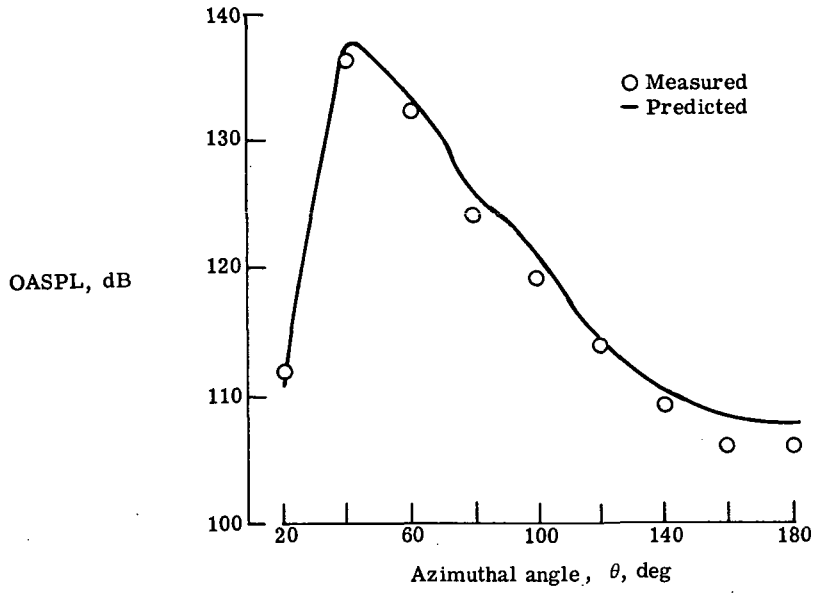

(a) Tunnel A.

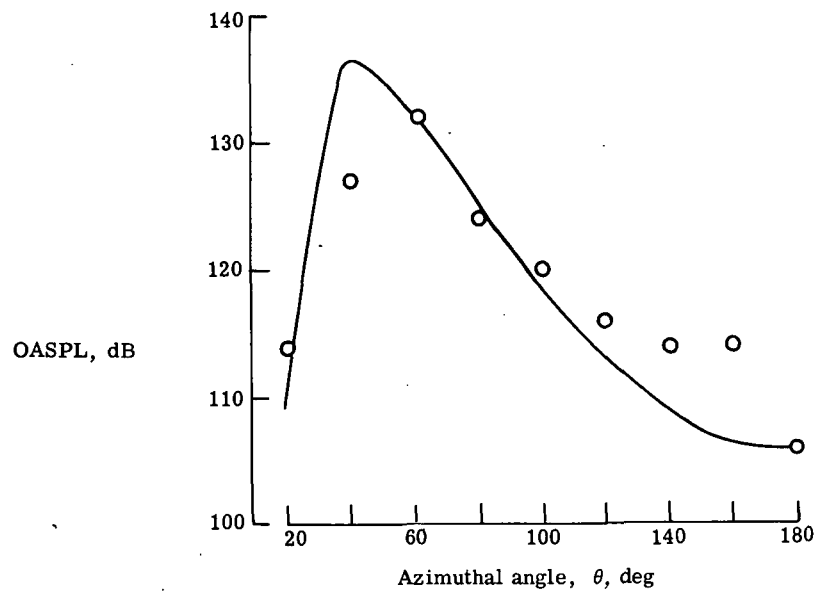

(b) Tunnel B.

Figure 11.- Comparison of predicted and measured OASPL.

Table II indicates that the external jet noise spectrum peak frequency occurs at 17 Hz and the external burner noise cut-off frequency is 11 Hz. If the jet noise is assumed to be the major contributor to the external noise field (since it is more than 12 dB above the burner noise), the predicted narrow band spectrum can be translated into a 1/3-octave

band spectrum as shown in the sample calculation. After incorporating atmospheric absorption effects, the predicted and measured spectra for tunnel B are shown in figure 12. Excepting the underprediction of the first spectrum peak, the predicted spectrum seems to envelop the external jet noise spectrum.

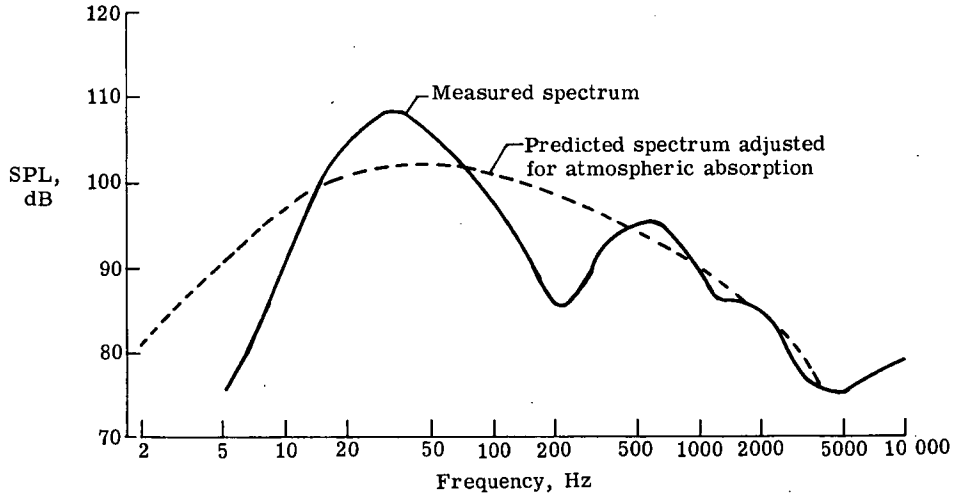

Figure 12.- Predicted and measured 1/3-octave band spectra at 304.8 m and 20° from tunnel B exit.

CONCLUDING REMARKS

A procedure for predicting the internal and external acoustic fields generated by blowdown wind tunnels has been systematized from the results of available empirical and theoretical studies. The external wind-tunnel OASPL and spectrum levels as predicted by this procedure compare favorably with existing experimental data.

The predictions of the TBL overall noise levels and spectrum shapes make use of empirical methods for which substantial data exist. However, no data were available with which to judge the validity of the test-section burner noise prediction techniques.

The wind tunnels used had the exhaust jet acting as the major external noise source. No data are available for tunnels in which the burner is the predominant external noise source.

Until more definitive wind-tunnel noise measurements are available, the prediction scheme seems to be a good first step in the development of a general blowdown wind-tunnel noise prediction capability.

Langley Research Center,
National Aeronautics and Space Administration,
Hampton, Va., April 25, 1972.

REFERENCES

1. Lowson, M. V.: Prediction of Boundary Layer Pressure Fluctuations. AFFDL-TR-67-167, U.S. Air Force, Apr. 1968. (Available from DDC as AD 832 715.)

2. Bies, David Alan: A Review of Flight and Wind Tunnel Measurements of Boundary Layer Pressure Fluctuations and Induced Structural Response. NASA CR-626, 1966.

3. Bushnell, K. W.: A survey of Low Velocity and Coaxial Jet Noise With Application to Prediction. J. Sound Vib., vol. 17, no. 2, July 22, 1971, pp. 271-282.

4. Von Gierke, Henning E.: Aircraft Noise Sources. Handbook of Noise Control, Cyril M. Harris, ed., McGraw-Hill Book Co., Inc., 1957, pp. 33-1 – 33-65.

5. Mayes, William H.; Edge, Philip M., Jr.; and O'Brien, James S., Jr.: Near-Field and Far-Field Noise Measurements for a Blowdown-Wind-Tunnel Supersonic Exhaust Jet Having About 475,000 Pounds of Thrust. NASA TN D-517, 1961.

6. Anon.: Jet Noise Prediction. AIR 876, Soc. Automot. Eng., July 10, 1965.

7. Kotake, Susumu; and Hatta, Keizo: On the Noise of Diffusion Flames. Bull. JSME, vol. 8, no. 30, 1965, pp. 211-219.

8. Strahle, Warren C.: On Combustion Generated Noise. AIAA Paper No. 71-735, June 1971.

9. Peterson, Arnold P. G.; and Gross, Ervin E., Jr.: Handbook of Noise Measurement. Sixth ed., General Radio Co., c.1967.

10. Anon.: Acoustic Loads Generated by the Propulsion System. NASA Space Vehicle Design Criteria (Structures). NASA SP-8072, 1971.

11. Sutherland, L. C., ed.: Sonic and Vibration Environments for Ground Facilities – A Design Manual. Rep. No. WR 68-2 (Contract NAS8-11217), Wyle Lab., Mar. 1968, p. 7-13. (Available as NASA CR-61636.)

"The aeronautical and space activities of the United States shall be conducted so as to contribute . . . to the expansion of human knowledge of phenomena in the atmosphere and space. The Administration shall provide for the widest practicable and appropriate dissemination of information concerning its activities and the results thereof."

—NATIONAL AERONAUTICS AND SPACE ACT OF 1958

NASA SCIENTIFIC AND TECHNICAL PUBLICATIONS

TECHNICAL REPORTS: Scientific and technical information considered important, complete, and a lasting contribution to existing knowledge.

TECHNICAL NOTES: Information less broad in scope but nevertheless of importance as a contribution to existing knowledge.

TECHNICAL MEMORANDUMS: Information receiving limited distribution because of preliminary data, security classification, or other reasons.

CONTRACTOR REPORTS: Scientific and technical information generated under a NASA contract or grant and considered an important contribution to existing knowledge.

TECHNICAL TRANSLATIONS: Information published in a foreign language considered to merit NASA distribution in English.

SPECIAL PUBLICATIONS: Information derived from or of value to NASA activities. Publications include conference proceedings, monographs, data compilations, handbooks, sourcebooks, and special bibliographies.

TECHNOLOGY UTILIZATION PUBLICATIONS: Information on technology used by NASA that may be of particular interest in commercial and other non-aerospace applications. Publications include Tech Briefs, Technology Utilization Reports and Technology Surveys.

Details on the availability of these publications may be obtained from:

SCIENTIFIC AND TECHNICAL INFORMATION OFFICE

NATIONAL AERONAUTICS AND SPACE ADMINISTRATION

Washington, D.C. 20546